IRANIAN JOURNAL OF CATALYSIS

Introducing Pt/ZnO as a new non carbon substrate electro catalyst for oxygen reduction reaction at low temperature acidic fuel cells

Rasol Abdullah Mirzaie*, Fatemeh Hamedi

Fuel Cell Research Laboratory, Department of Chemistry, Faculty of Sciences, Shahid Rajaee Teacher Training University, Tehran, Iran.

Received 18 March 2015; received in revised form 22 May 2015; accepted 26 May 2015

ABSTRACT

Gas diffusion electrode was used for providing better conditions in fuel cell systems for oxygen reduction reaction (ORR). Because the slow kinetics of the oxygen reduction reaction at the proton exchange membrane fuel cell cathode restricts fuel cell efficiency. To this end, researchers have used platinum-coated carbon. In the present study, due to the reduction of carbon corrosion, Zinc oxide nanoparticles have been employed as a support material for platinum. The Pt/ZnO nanoparticles catalyst was made via a combined process of impregnation and seeding method. The microstructure of coating was characterized using scanning electron microscopy (SEM) which indicates that Pt nanoparticles are uniformly dispersed on the surface of ZnO. In order to investigate the chemical composition and crystalline phases of coating, X-ray analysis was carried out. Electrochemical Impedance Spectroscopy (EIS) was carried out for comparing the charge transfer effect during the ORR. The catalytic performance of the electrodes for ORR is evaluated through linear sweep voltammetry measurement. The O_2 reduction current for Pt/ZnO alone is expectedly low due to the low electronic conductivity in ZnO. However, adding single-wall carbon nanotube (SWCNT) to the reaction layer improves the electrode performance. The prepared Pt/ZnO/SWCNT 30 wt. % electrode shows high catalytic activity for the ORR, which is probably attributed to conductivity changes caused by the addition of SWCNT. The electrochemical active surface area (ECSA) and durability investigation was studied by cyclic voltammetry in nitrogen saturated 0.5 M H_2SO_4. The results calculated from ECSA measurements were indicated that the degradation rate of optimized electrode is smaller than Pt/C electrode.

Keywords: *Oxygen reduction reaction; Gas diffusion electrode; Platinum on zinc oxide electrocatalysts; Catalytic activity; Non-carbon substrate; Single wall carbon nanotube.*

1. Introduction

Polymer electrolyte membrane fuel cells(PEMFCs) have long been thought of as a promising clean energy electrochemical device. They have some advantages, such as high power density, high efficiency, clean utilization and zero emission for promising green power sources [1-7]. But, fuel cell technologies have failed to reach mass commercialization mainly due to short operational lifetimes and the high cost of materials. In particular, the polymer membrane and the catalyst layer have been problematic in reducing the material cost. Among pure metals, platinum (Pt) is the best and most used cathode electro catalyst for oxygen reduction reaction (ORR) in low-temperature fuel cells due to its high activity and excellent chemical stability to produce high catalytic activity. Of course, Pt has a high cost and this problem is a barrier in the way of trading fuel cells [1,3, 8, 12-17]. The activity of cathode catalyst is very important for ORR of fuel cells since the sluggish kinetics of the ORR are typically attributed to the strength of the O=O bond (498 kJ/mol) that must be broken in the course of the reaction [8-11].

The catalytic oxygen reduction reaction on Pt in acidic media has been investigated by a number of researchers. Oxygen is reduced by two pathways: the direct 4-electron reduction pathway from O_2 to H_2O, and the 2-electron reduction pathway from O_2 to hydrogen peroxide (H_2O_2). The mechanism of the ORR on Pt in acidic medium followed the four-electron pathway. This process is quite complicated and

*Corresponding author email: ra.mirzaei@srttu.edu, mirzai_r@yahoo.com
Tel: +98 21 2297 0005; Fax: +98 21 2297 0005

involves different reaction intermediates. In this mechanism, O_2 can be reduced directly to water (direct 4-electron reduction) electrochemically, or adsorbed into hydrogen peroxide (H_2O_2, ad) with 2-electron reduction. H_2O_2,ad can be further reduced to water, chemically decomposed on the electrode surface, and/or desorbed into the electrolyte solution [18].

The most used support for preparing fuel cell catalysts is carbon black (Vulcan Xc-72) because of its good electron conductivity and surface area [19]. One major problem in catalyst is carbon corrosion and the presence of platinum on carbon increases rate of carbon corrosion [5, 20-22]. The performance of the catalyst supports improved with the use of nanostructured carbon materials because they show strong influence on the catalyst durability and behavior. So electro catalyst support materials with low-cost, high-performing and non-corrosive properties are required. Therefore, in this study non-carbon substrate has been used to decrease carbon corrosion. Interactions between the catalyst and the support enhance catalyst efficiency and reduce catalyst loss; furthermore, they control charge transfer. The support can also help enhance the catalyst performance, although the kind of support material is very important for determining the performance, life and cost of the catalyst and the overall fuel cell [20].

In recent years, the use of the metal oxides substrate for preparation of fuel cell electro catalyst has been investigated. For instance, TiO_2 [23-27], SiO_2 [28], NbO_2 [29], SnO_2 [30,31] and WO_x [11,26,32-34] have been studied for preparation cathode catalyst in fuel cell systems and induced an enhancement of the catalytic activity probably induced by the strong metal support interaction(SMSI) effect.

Camacho has prepared a series of oxide-carbon composites using different oxides (TiO_2, SnO_2, ZnO) and a selective platinum deposition onto the oxide sites to obtain Pt/TiO_2-C, Pt/SnO_2-C and Pt/ZnO-C was carried out. They found that the Pt/oxide-carbon materials showed higher ORR activity than Pt/C catalyst [35].

Supported catalyst systems have been used as they represent a hopeful category of electro catalyst; in addition to the enhancement of real surface area, strong metal support interaction (SMSI) can also be found in supported catalyst systems such an effect was reported in titanium/platinum system[20,26,36].

One of the most commonly used methods to prepare catalysts is impregnation [37]. In this technique, a certain volume solution containing the precursor of the active element of the catalyst is contacted with the solid support [38]. Support can be impregnated with catalyst precursors by mixing the two in an aqueous solution. A reduction step is needed for following the impregnation step to reduce the catalyst precursor to its metallic state [37].

Thus, according to the above-mentioned problems and previous studies, this paper is focused on the improvement of ORR kinetics and on the approach of non-carbon substrate in the preparation of electro catalyst and disadvantages of carbon support. The use of ZnO as a substrate has attracted interest because zinc oxide is one of the most important semiconductor material with direct band gap(3.37 ev or 375nm), good transparency and high electron mobility (>100 $cm^2/v.s$). It has attracted increasing attention due to excellent electrical properties, inexpensiveness, relative abundance, chemical stability towards air, the specific morphology (nanorod), higher surface area,(23 $m^2.g^{-1}$), and high dispersion in solution [39-44]. Since ZnO is an important trace element for humans, it is environment-friendly and suitable for in vivo application. It could be assumed that ZnO can act as a good substrate for cathode catalyst in PEMFC. In order to optimize the structure of prepared electro catalyst, the effect of SWCNT addition to the reaction layer according to its electrical conductivity was studied.

In this research, the low temperature synthesis associated with the combined processes of impregnation and seeding was used to prepare Pt/ZnO electro catalysts for the oxygen reduction reaction in PEM fuel cells. The effects of ORR kinetics of these as-prepared electro catalysts were investigated.

2. Experimental

2.1. Synthesis of nano ZnO powder

All chemicals were purchased from Merck and used as received without further purification. The preparation of nano ZnO powder is described as follows: First, 1.0 mmol Zn $(CH3COO)_2 \cdot 2H_2O$ was poured in an agate mortar. Then, 4 mmol NaOH was added to the sample and ground for 60 min at room temperature. Finally, the white mixture was transferred to a beaker and washed fully with distilled water and ethanol for several times and dried at room temperature [39].

2.2. Electro catalyst preparation

At first the 0.00193 M Pt solution was obtained by H_2PtCl_6 (Fluka) and then the solution pH was adjusted with 1 M NaOH, as required, to the desired value. The zinc oxide slurry was prepared by dispersing of 2.26 mg of Zinc oxide in de-ionized water, sonicating for 10 min and mixing approximately 10% (v/v) of the Pt solution with the zinc oxide slurry and sonicating for 30 min. To prepare the seeded electro catalyst, the seeded powder was obtained by the reduction of the previous solution with 0.1 M $NaBH_4$, sedimented by centrifugation and the pellet was harvested and dried

by oven. Thereafter, the obtained powder was dispersed, in de-ionized water, sonicating for 30 min and the remaining Pt solution (90%) was added to the required metal loading on zinc oxide substrate. To obtain the catalyst powder, which was settled from the solution, the mixture was again reduced with 0.1 M $NaBH_4$. The electro catalyst solution was filtered, washed thoroughly with de-ionized water and dried by oven for 7 hours at 110 °C [45].

2.3. Fabrication of gas diffusion electrodes

For fabrication the electrode, the catalyst ink was obtained from mixing1.0 ml of 2-propanol, 1ml distilled H_2O with 30 wt.% of polytetrafluoroethylene solution and 3 mg of electrocatalyst, sonicating them at room temperature for 30 min to obtain the ink which was then coated onto a carbon paper and dried at 200°c for 60 min. This electrode is labeled Pt/ZnO. The electrodes were fabricated at various contents of single wall carbon nanotube (SWCNT) [45].

2.4. Physical characterization

XRD is often used to identify what elements a heterogeneous mixture is composed of, the crystalline structure of those elements, as well as the crystallite size or grain size. The X-ray diffraction equipment usually controls the position of the X-ray beam (incident ray) and the position of the detector (reflected ray) and records the observed intensity at the detector. In this way, a plot called a diffractogram is obtained with the angle in 2θ on the x-axis versus intensity which is plotted on the y-axis [46].The X-ray diffractograms were recorded using a Cu Kα source radiation in an equinox diffractometer and operating in the symmetry geometry. The diffractometer was operated in the step scan mode with a 0.03 step and in the range of 5-118º (2Θ). The high tension generator, Equinox3000 was operating at 40 Kv and 30 mA. Scanning electron microscopy (SEM) is a well-known physical characterization technique that is utilized for observing the morphology of a sample at high magnification. SEM can be coupled with energy dispersive X-ray (EDX) analysis to determine elemental composition as well as other properties such as electro conductivity of a sample. The device takes advantage of electrons having a particular wavelength to act like photons [47]. EDX and SEM analysis was carried out using a VEGAⅡ SEM.

2.5. Electrochemical measurement

The electrochemical experiments were performed at 27°C using a potentiostat (Zahner). A conventional three-electrode cell was used in linear sweep voltammetry (LSV) and Electrochemical Impedance Spectroscopy (EIS). All the electrode potentials in this work are related to the reference Ag/AgCl electrode in a 0.5 M H_2SO_4 aqueous solution electrolyte.The working electrode was amount of synthesized electro catalyst powder that was coated on Carbon paper and Pt electrode as a counter electrode was used. Linear sweep voltamograms (lsv) were recorded from 0.8 to -0.2 V vs. Ag/AgCl in oxygen saturated electrolyte. Cyclic voltammetry (CV) is the experimental technique to durability investigation and determinate electrochemical active surface area (ECSA), that is in nitrogen saturated 0.5M H_2SO_4 electrolyte from 0.8 to -0.2 V at 50 $mv.s^{-1}$scan rate by integrating the hydrogen adsorption-desorption region using EQ (1). Where L_{Pt} is the platinum loading ($mg.cm^{-2}$) in the electrode, Q_H is the charge for hydrogen desorption ($mC.cm^{-2}$) and Q_F =0.21 $mC.cm^{-2}$ represents the charge required to oxidize a monolayerof H_2 on bright Pt [35,48,49].

$$\text{ECSA} = \frac{Q_H}{L_{Pt} \times Q_F} \quad (1)$$

Electrochemical Impedance Spectroscopy (EIS) is an experimental technique that can be applied in-situ to separate the physical processes in the PEFC which occur at different rates through a frequency response plot. The resulting impedance is commonly shown in a complex plane and represents the electrochemical and diffusion mechanisms of the PEFC in the frequency domain. The impedance spectrum mainly represents the charge transfer effect during the ORR and its diameter decreases with increasing current density [50,51]. This technique was used and Nyquist plots were recorded from100 kHz to 10 mHz frequency.

3. Results and discussion

3.1. XRD analysis of Pt/ZnO electrocatalyst

XRD analysis of Pt on zinc oxide substrate nanoparticles is shown in Fig. 1, that reveals the characteristic (111), (200), (220) and (311) reflections of face centered cubic crystalline Pt at 2θvalues of 39.6° , 46.1° , 67.2° and 81.8°, respectively as described elsewhere. As reported in a previous article [39], Major ZnO hexagonal wurtzite structure (JCPDS 36-1451) is observed in XRD pattern and (100),(002),(101),(102),(110),(103) and (112) reflection of zinc oxide are located at 31.84°, 34.52°, 36.33°, 47.63°, 56.71°, 62.96°, and 68.13°, respectively. XRD pattern demonstrates that the produced product shows a high-quality wurtzite ZnO structure, as shown in Fig.1 [52]. From this XRD patterns the particle size of the sample was determined. It was calculated using Debye-Scherrer formula [46] EQ (2):

$$d = \frac{0.89\,\lambda}{\beta\,cos\theta} \quad (2)$$

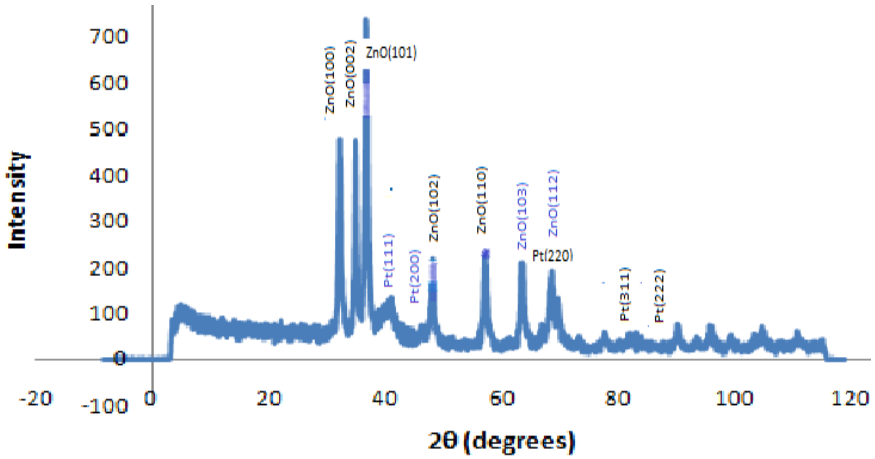

Fig. 1. XRD patterns of Pt/ZnO powder prepared by solid-state reaction at room temperature.

where 0.89 is Scherrer's constant, λ is the wavelength of X-rays, θ is the Bragg diffraction angle, and β is the full width at half-maximum (FWHM) of the diffraction peak corresponding to plane <101>. The average particle size of the sample was obtained to be 20.66 nm which is derived from more intense peak corresponding to 101 plane located at 36.33°.

3.2. SEM characterization of Pt/ZnO electrocatalyst

Fig.2A shows the SEM image of pure ZnO prepared by the solid state reaction. From this image short ZnO nanorods are observed [39]. The SEM images of Pt/ZnO/SWCNT 30wt.% are also shown in Fig. 2B and C at different magnifications. The white and bright points are the platinum particles.The presence of Pt, ZnO and CNT was confirmed by using energy dispersive X-ray (EDX) spectrum. Mapping images are showed in Fig. 3 for Pt/ZnO/SWCNT 30wt. % electrode. It can be seen that the platinum nanoparticles are uniformly distributed on ZnO substrate.

3.3. Study of Pt/ZnO electro catalyst for ORR

In this research, ZnO nanoparticles was used as a substrate for platinum and prepared Pt/ZnO electro catalyst instead of Pt/C.

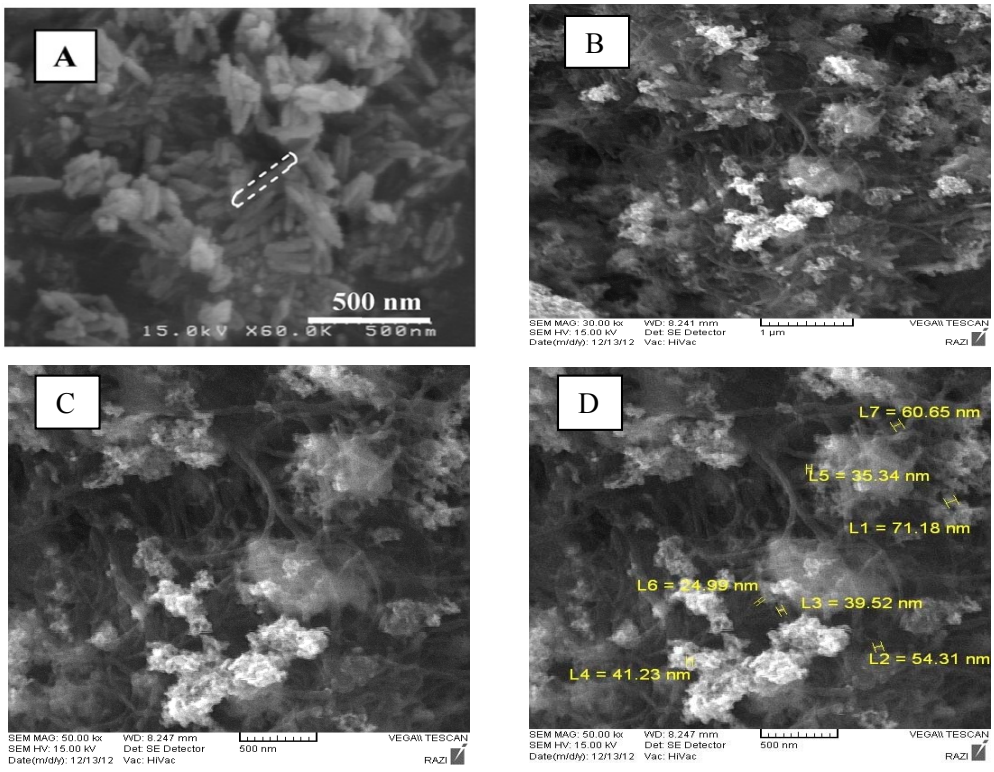

Fig. 2. SEM images of (A) pure ZnO [39], (B) and (C) Pt/ZnO/SWCNT 30wt.% electrocatalyst at 30000X and 50000X magnifications, (D) indicates the size of nanoparticles.

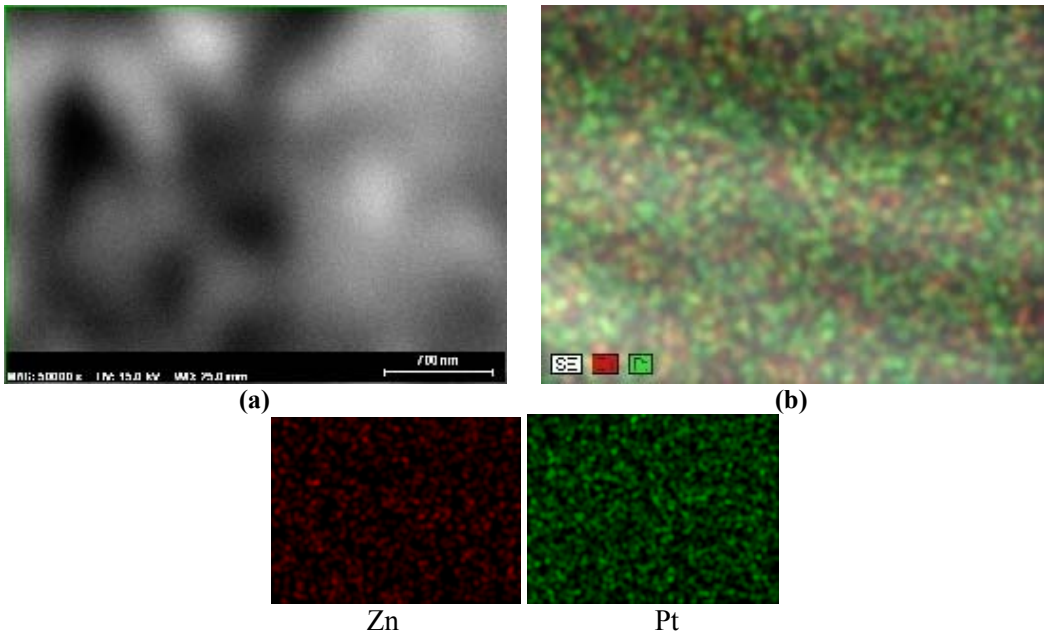

Fig. 3. SEM image (a) and map data (b) of Pt/ZnO/SWCNT 30wt. % electrocatalyst.

3.3.1. E/I response

Fig. 4. depicts the linear sweep voltamograms (lsv) for commercial Pt/C and Pt/ZnO catalysts in O_2 saturated 0.5M H_2SO_4 solution obtained at scan rate of 1 mV/s. As can be seen in diagrams with alternating the substrate, efficiency is reduced. This is due to the low conductivity of ZnO because ZnO is a semiconductor. It can be improved by addition amounts of SWCNT in the reaction layer.

3.4. Optimization of Pt/ZnO electrocatalyst performance at a range of SWCNT concentration

As can be seen in diagrams, with alternating the substrate from carbon to zinc oxide, efficiency was reduced but it can be optimized by adding a range of SWCNT concentration.

3.4.1. ORR kinetics

Using the same catalyst loading under the same conditions for Pt/ZnO, Pt/ZnO/SWCNT 10 wt. %, Pt/ZnO/SWCNT 20 wt. %, Pt/ZnO/SWCNT 30 wt. %, Pt/ZnO/SWCNT 40 wt. %, Pt/ZnO/SWCNT 50 wt. % electrodes. These electrodes were studied in 0.5 M H_2SO_4 and at 27°C in a three electrode cell for oxygen reduction reaction. Linear sweep voltammetry (LSV) experiments were used to investigate the electrochemical activity for ORR. At the beginning of the experiments, the solution was purged with O_2 for 30 min. The scanning potential was from 0.8 to -0.2 V versus Ag/AgCl with a scan rate of 1 $mV.s^{-1.}$ The polarization curves are shown in Fig. 5. All of the curves to the potential of 0.8 V vs SHE are approximately located.

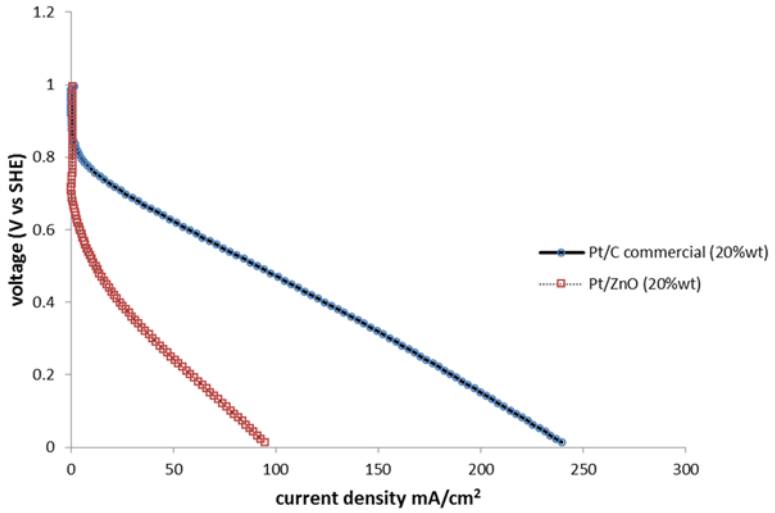

Fig. 4. Comparison of polarization curves between Pt/ZnO and commercial Pt/C 20wt.% recorded in O_2-saturated 0.5 M H_2SO_4 solution at 27°C. Potential scan rate: 1 mV/s.

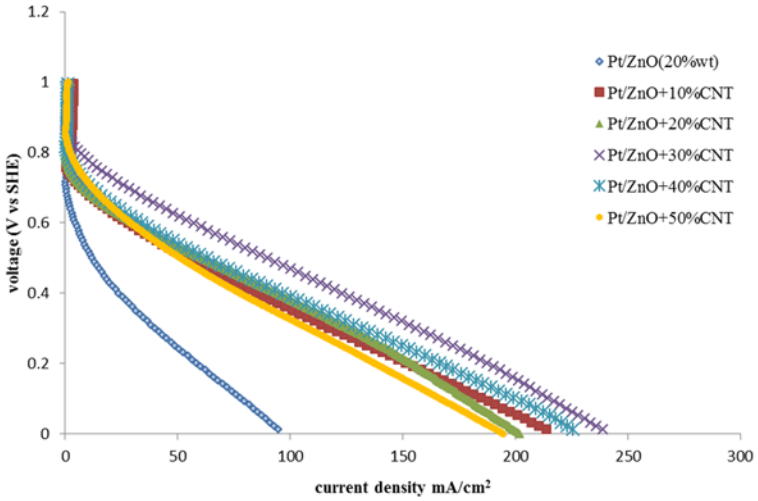

Fig. 5. Linear potential sweep curves of ORR on different electrodes for oxygen reduction in O_2 saturated 0.5 M H_2SO_4 solution at potential scan rate of 1 mV/s and 27°C.

As it can be seen, the ORR current is increasing with decreasing the potential for all of them but the slope of the polarization curve for the electrode containing 30 wt. % SWCNT was larger than the others; therefore, the surface of this electrode is more appropriate for oxygen reduction reaction and its electrochemical activity for ORR is higher. The mentioned electrode displayed higher catalytic performance for ORR because its reduction potential at any reduction current is upper than the others. This graph shows that the efficiency can be increased by adding carbon nanotubes. SWCNT will lead to an increase in conductivity of electrode and it can be assumed that the pore structure of the catalyst layer was significantly improved by the SWCNT at optimized value. Hence the existence of additive in the catalyst layer affects the performance of catalyst layer for ORR. However it cannot be stated clearly about the effect of SWCNT.

3.4.2. Exchange current density

Exchange current density (i_0) measurements for oxygen reduction have been carried out by using linear sweep voltammetry method. The i_o values were obtained and listed in table1. The results for Pt/C catalyst is 57.851 mA.cm^{-2}, whereas for Pt/ZnO catalyst with 30wt. % SWCNT is 70.885 mA.cm $^{-2}$ that shows Pt/ZnO /SWCNT possess a greater catalytic activity than carbon used in Pt/C.

3.4.3. E/I response

As listed in Table 1, 700mV is measure of the kinetics, measure of the ohmic drop is 500mV and 300mV is a measure of the concentration polarization .As can be seen in the range of kinetics, results are closer together and in the concentration range the results are far. Furthermore, the electrode containing 30 wt. % carbon

Table 1. Values of exchange current density and current density of Pt/ZnO electrocatalyst with various carbon nano tube concentration.

Electrocatalyst	Exchange current density; i_0 (mA/cm^2)	Current density in 300 mV (mA/cm^2)	Current density in 500 mV (mA/cm^2)	Current density in 700 mV (mA/cm^2)
Pt/ZnO (20 wt. %)	20.17	43.3	14	0.9
Pt/C (commercial) 20 wt. %	57.85	162	97.6	29.9
Pt/ZnO/SWCNT 10 wt. %	54.15	124	61	9.16
Pt/ZnO/SWCNT 20 wt. %	66.15	132	67	9.58
Pt/ZnO/SWCNT 30 wt. %	70.88	163	96.7	31
Pt/ZnO/SWCNT 40 wt. %	56.93	139	69.3	14
Pt/ZnO/SWCNT 50 wt. %	40.59	114	56.1	13.8

nanotubes has a good kinetics and acts better than others. Therefore, the optimized electrode is Pt/ZnO/SWCNT 30 wt. %.

3.4.4. Electrochemical impedance spectroscopy (EIS) studies of the electrodes

EIS studies can complete polarization analysis to investigate electrodes behavior. These measurements were carried out in O_2 saturated aqueous solution of 0.5 M H_2SO_4, at 27°C and at potential of 0.5 V. The Nyquist plots of EIS measurements were recorded by sweeping frequencies over the range of 100 kHz-10 mHz. They are shown in Fig. 6. As can be seen, all three plots have a semi-circle form. The diameter of these semi-circles display the charge transfer resistance indicating catalytic activity for ORR. This figure shows that with adding SWCNT, the diameter of the semi-circle in electrode containing 30 wt. % SWCNT is much smaller. Therefore, the charge transfer resistance is dramatically reduced. It is comparable with the diameter of the semi-circle in commercial Pt/C electrode.

3.5. Electrochemical stability performance

An important factor in the characterization of Ptelectrocatalysts is the electrochemical active surface area (ECSA) which was determined from CV data in the hydrogen adsorption-desorption region using EQ (1). The CVs for Pt/ZnO/SWCNT 30wt.% and commercial Pt/C 20wt.% catalysts were recorded before and after 1200 potential cycles. Good hydrogen adsorption/desorption peaks appeared in Fig.7. During the negative going potential sweep, a reduction peak can be seen which can be attributed to the reduction of platinum oxide. The ECSA measurements were carried out during the potential cycling test for investigating durability of Pt/ZnO and Pt/C catalysts. The potential cycles were from 0.8 to -0.2 V vs Ag/AgCl at 50 $mV.s^{-1}$ in 0.5 $mol.L^{-1}H_2SO_4$. ECSA ($m^2g^{-1}{}_{Pt}$) of the catalysts were obtained from the columbic charge for the hydrogen adsorption and desorption (Q_H) in the cyclic voltammograms (Figs. 7a,b). The value of Q_H is calculated as the mean value between the amounts of charge transfer during the electro-adsorption and desorption of H_2 on Pt sites [53].

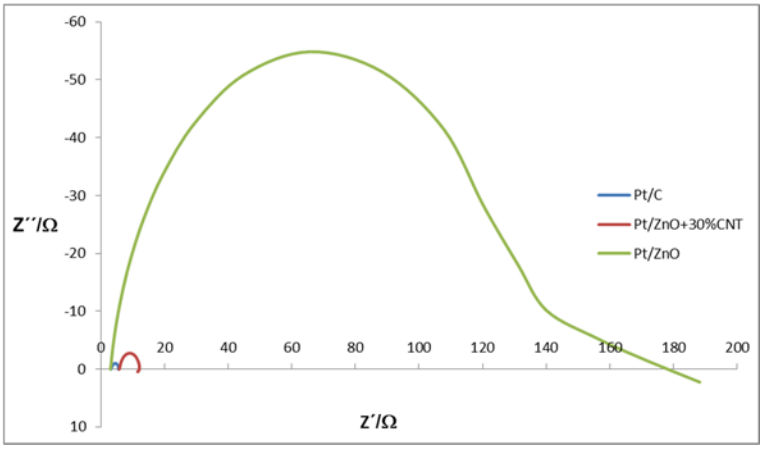

Fig. 6. Comparison of nyquist diagrams between Pt/ZnO, Pt/ZnO/SWCNT 30wt.% and commercial Pt/C 20 wt. % electrocatalysts from 100kHz to 10 mHz, in O_2-saturated 0.5 M H_2SO_4 solution at 0.5V vs Ag/AgCl electrode and 27°C.

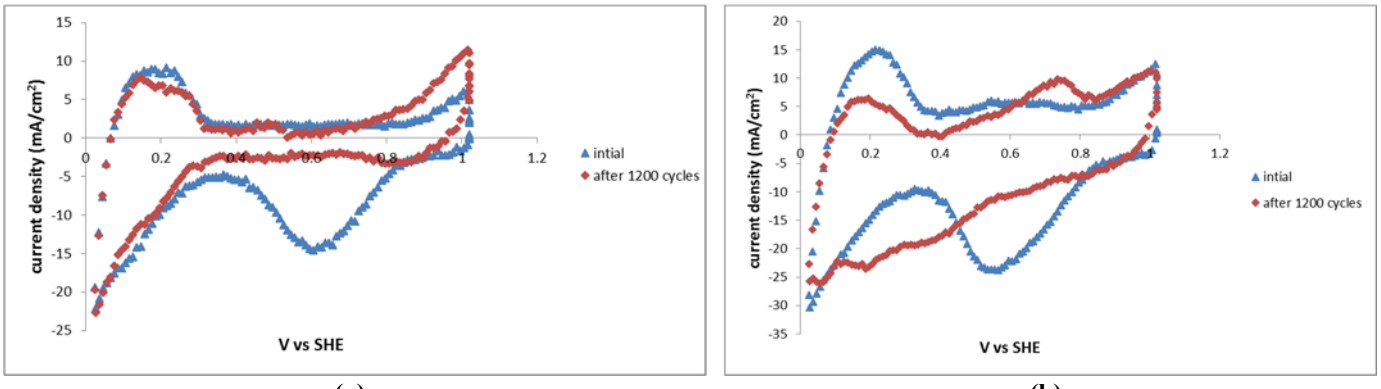

(a) **(b)**

Fig. 7. Cyclic voltammgrams recorded on Pt/ZnO/SWCNT 30 wt. % (a) and commercial Pt/C (20wt.%) (b) electrodes before and after 1200 potential cycles, scan rate: 50 mVs^{-1}, temperature: 27 °C.

Fig. 8 shows the ECSA as a function of the cycle number obtained for Pt/ZnO and Pt/C catalysts. As can be seen, the initial ECSA of Pt/C 20 wt. % before potential cycling test is expectedly higher than that of Pt/ZnO/SWCNT 30 wt. %. In addition, Table 2 shows the amounts of ECSA before and after 1200 potential cycles, the ECSA for commercial Pt/C decreases from 84.21 to 31 $m^2.g^{-1}$ Pt (by 63.18%) and for Pt/ZnO/SWCNT 30 wt. % from 46.79 to 37.97 (by 18.85%). Therefore the degradation rate of the Pt/C catalyst is larger than that of the Pt/ZnO catalyst.

4. Conclusions

To summarize, ZnO nanoparticles has been synthesized by a simple solid-state reaction method and it has been used as cathode catalyst support. Pt/ZnO catalyst was prepared via a combined process of impregnation and seeding method instead of Pt/C. In fact, in this work non-carbon substrate (ZnO nanoparticles) for platinum was used to optimize application of zinc oxide for support material in oxygen reduction reaction. ZnO was chosen because it can be easily manufactured at low cost and Zn is a transition metal and has the orbitals that can establish a strong link with Pt *d* orbitals. This prevents detachment of the platinum from the substrate. The results show that ZnO as a substrate can be used for Pt electro catalyst instead of carbon that provides a new kind of cost-effective support with corrosion resistance for deposition Pt nanoparticles. To optimize the electro-catalyst prepared by zinc oxide, the carbon nanotubes were mixed in the reaction layer. The presence of SWCNTs along with zinc oxide makes a condition in which electrode performance is optimized. It can be guessed that it can enhance the electrode conductivity as shown in impedance results as others have observed good effects. The Pt/ZnO/SWCNT 30wt.% showed high catalytic activity for oxygen reduction reaction in acidic media, which could be attributed to the unique nanostructure of the catalysts, highly distributed Pt nanoparticles and electrochemical stability performance. Thus, based on exchange current density (i_0) measurements, it can be concluded that the mentioned electrode has faster kinetics, better performance and it quickly responds to changing potential.

Acknowledgment

The authors would like to acknowledge the support of the Fuel Cell Research laboratory of Shahid Rajaee Teacher Training University (Tehran, Iran).

References

[1] H. Zhu, M. Luo, S. Zhang, L. Wei, F. Wang, Z. Wang, Y. Wei, K. Han, Int. J. Hydrogen Energy 38 (2013) 3323-3329.

[2] S.M Andersen, M. Borghei, P. Lund, Y. Elina, A. Pasanen, E. Kauppinen, V. Ruiz, P. Kauranen, E.M. Skou, Solid State Ionics 231 (2013) 94–101.

[3] B.N. Popov, X. Li, G. Liu, J.W. Lee, Int. J. Hydrogen Energy 36 (2011) 1794-1802.

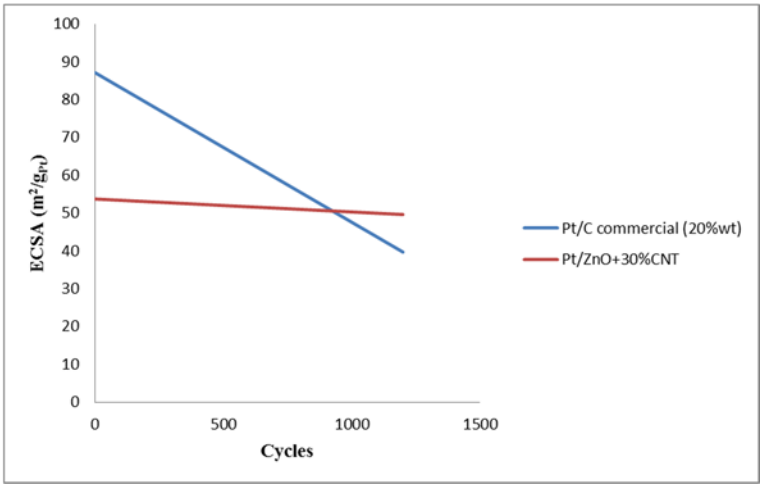

Fig. 8. Electrochemical active surface area as a function of cycle numbers on Pt/ZnO/SWCNT 30wt.% and commercial Pt/C (20wt.%) electrodes.

Table 2. Comparison of prepared electrodes (commercial Pt/C (20wt.%) and Pt/ZnO/SWCNT 30wt.%)for catalyst degradation.

Catalyst	ECSA (m^2/g_{Pt})	
	Initial	After 1200 cycles
Pt/C commercial wt.20%	84.21	31
Pt/ZnO/SWCNT 30wt.%	46.79	37.97

[4] W. Song, H. Yu, L. Hao, Z. Miao, B. Yi, Z. Shao, Solid State Ionics 181 (2010) 453–458.
[5] B. Zhao, L. Sun, R. Ran, Z. Shao, Solid State Ionics 262 (2014) 313–318.
[6] B. Li, Z. Yan, D.C. Higgins, D. Yang, Z. Chen, J. Ma, J. Power Sources 262 (2014) 488-493.
[7] H. Zhang, P.K. Shen, Chem. Soc. Rev. 41 (2012) 2382-2394.
[8] J. Bai, Q. Zhu, Z. Lv, H. Dong , J. Yu, L. Dong, Int. J. Hydrogen Energy 38 (2013) 1413-1418.
[9] A. Maghsodi, M.R. Milani Hoseini, M. Dehghani Mobarakeh, M. Kheirmand, L. Samiee, F. Shoghi, M. Kameli, Appl. Surf. Sci. 257 (2011) 6353–6357
[10] H.H. Wang, Z.Y. Zhou, Q. Yuan, N. Tian, S.G. Sun, Chem. Commun. 47 (2011) 3407–3409.
[11] M.S. saha, Y. Zhang, M. Cai, X. Sun, Int. J. Hydrogen Energy 37 (2012) 4633-4632.
[12] C.H. Chang, T.S. Yuen, Y. Nagao, H. Yugami, Solid State Ionics 197 (2011) 49–51.
[13] I. Gatto, A. Stassi, E. Passalacqua, A.S. Arico, Int. J. Hydrogen Energy 38 (2013) 675-681.
[14] L-R. Yang, D-S. Tsai, Y-S. Chao, W-H. Chung, D.P. Wilkinson, Int. J. Hydrogen Energy 36 (2011) 7381-7390.
[15] R. Wang, X. Li, H. Li, Q. Wang, H. Wang, W. Wang, J. Kang, Y. Chang, Z. Lei, Int. J. Hydrogen Energy 36 (2011) 5775-5781.
[16] K-S. Lee, C. Jang, D. Kim, H. Ju, T-w. Hong, W. Kim, D. Kim, Solid State Ionics 225 (2012) 395–397.
[17] S.S. Jyothirmayee, S. Ramaprabhu, ACS Appl. Mater. Interfaces 4 (2012) 3805−3810.
[18] N.M. Markovic, P.N. Ross, Surf. Sci. Rep. 45 (2002) 117-229.
[19] Y. Lin, X, Cui, C. Yen, C.M. Wai, J. Phys. Chem. B 109 (2005) 14410 14415.
[20] S.G. Sharma, B. Pollet, J. Power Sources 208 (2012) 96-119.
[21] B. Avasarala, P. Haldar, Int. J. Hydrogen Energy 36 (2 0 1 1) 3965-3974.
[22] S. Yin, S. Mu, M. Pan, Z. Fu, J. Power Sources 196 (2011) 7931– 7936.
[23] S.V. Kraemer, K. Wikander, G. Lindbergh, A. Lundblada, A.E.C. Palmqvist, J. Power Sources 180 (2008)185-190.
[24] T. Ioroi, Z. Siroma, N. Fujiwara, S.I. Yamazaki, K. Yasuda, Electrochem. Commun. 7 (2005) 183-188.
[25] G. Chen, C.C. Waraksa, H. Cho, D.D. Macdonald, T.E. Mallouka, J. Electrochem. Soc. 150 (2003) E423-E428.
[26] L. Timperman, A. Lewera, W. Vogel, N. Alonso-Vante, Electrochem. Commun. 12 (2010) 1772-1775.
[27] K.W. Park, K.S.Seol, Electrochem. Commun. 9 (2007) 2256–2260.
[28] B. Seger, A. Kongkanand, K. Vinodgopal, P.V. Kamat, J. Electroanal. Chem. 621 (2008) 198-204.
[29] K. Sasaki, L. Zhang, R. Adzic, Phys. Chem. Chem. Phys. 10 (2008) 159-167.
[30] M. Dou, M. Hou, D. Liang, W. Lu, Z. Shao, B. Yi, Electrochim. Acta 92 (2013) 468– 473.
[31] S.A. Jina, K. Kwon, C. Pak, H. Chang, Catal. Today 164 (2011) 176–180.
[32] J. Shim, C.R. Lee, H.K. Lee, J.S. Lee, E.J. Cairns, J. Power Sources 102 (2001) 172-177.
[33] H. Chhina, S. Campbell, O, Kesler, J. Electrochem. Soc. 154 (2007) B533–B539.
[34] M.S. Saha, M.N. Banis, Y. Zhang, R. Li, X. Sun, M. Cai, F.T. Wagner, J. Power Sources 192 (2009) 330-335.
[35] B.R. Camacho, C. Morais, M.A. Valenzuela, N. Alonso-Vante, Catal. Today 202 (2013) 36-43.
[36] S.J. Tauster , S.C. Fung, R.L. Garten, J. Am. Chem. Soc 100 (1978) 170-175.
[37] X.-Z. yuan, H. wang, PEM fuel cell electrocatalysts and catalyst layers: fundamentals and applications, in: J. Zhang (Ed.), PEM Fuel Cell Fundamentals, Springer, Vancouver, Canada, 2008, pp. 89-134.
[38] J.A. Schwarz, C. Contescu, A. Contescu, Chem. Rev. 95 (1995) 477-510.
[39] R. Abdullah Mirzaie, F. Kamrani, A. Anaraki Firooz, A.A. Khodadadi, Mater. Chem. Phys. 133 (2012) 311-316.
[40] E.V. Ramos-Fernandez, A. Sepulveda -Escribano, F. Rodrıguez-Reinoso, Catal. Commun. 9 (2008)1243-1246.
[41] N. Tamaekong, C. Liewhiran, A. Wisitsoraat, S. Phanichphant, Sensor. Actuat B: Chem. 152 (2011) 155–161.
[42] M. Consonni, D. Jokic, D.Y. Murzin, R. Touroude, J. Catal. 188 (1999) 165–175.
[43] M. Ohta, Y. Ikeda, A. Igarashi, Appl. Catal. A 258 (2004) 153–158.
[44] S.K. Mishra, R.K. Srivastava, S.G. Prakash, J. Alloy. Compd. 539 (2012) 1–6.
[45] W. Trongchuankij, K. Pruksathorn, M. Hunsom, Appl. Energy 88 (2011) 974-980.
[46] B. Cullity, S. Stock, Elements of X-ray Diffraction, Addison-Wesley Reading, MA, 1978.
[47] C. Jeffree, N.D Read, "Ambient- and Low-temperature scanning electron microscopy". In Hall, J. L. and Hawes, C. R. Electron Microscopy of Plant Cells. London: Academic Press. (1991) 313–413.
[48] W. Zhang, J. Chen, G.F. Swiegers, Z-F. Ma, G.G. Wallace. Nanoscale 2 (2010) 282–286.
[49] A. Pozio, M.D. Francesco, A. Cemmi, F. Cardellini, L. Giorgi, J. Power Sources 105 (2002) 13–19.
[50] S. Cruz-Manzo, R. Chen, P. Rama, Int. J. Hydrogen Energy 38 (2013) 1702-1713.
[51] G. Chen, C.C. Waraksa, H. Cho, D.D. Macdonald, T.E. Mallouka, J. Electrochem. Soc. 150 (2003) E423-E428.
[52] S. Talam, S.R. Karumuri, N.Gunnam. ISRN Nanotechnology 372505 (2012) 1-6.
[53] J. Wang, G. Yin, Y. Shao, S. Zhang, Z. Wang, Y. Ga, J. Power Sources 171 (2007) 331–339.